Effect of hydrophobic mismatch on domain formation and peptide sorting in the multicomponent lipid bilayers in the presence of immobilized peptides

ARTICLE *in* THE JOURNAL OF CHEMICAL PHYSICS · AUGUST 2014

Impact Factor: 2.95 · DOI: 10.1063/1.4891931 · Source: PubMed

3 AUTHORS, INCLUDING:

Qing Liang
Zhejiang Normal University
10 PUBLICATIONS **44** CITATIONS
SEE PROFILE

Zhi Yong Wang
Chongqing University of Technology
22 PUBLICATIONS **194** CITATIONS
SEE PROFILE

Effect of hydrophobic mismatch on domain formation and peptide sorting in the multicomponent lipid bilayers in the presence of immobilized peptides

Qing Liang, Qing-Yan Wu, and Zhi-Yong Wang

Citation: The Journal of Chemical Physics **141**, 074702 (2014); doi: 10.1063/1.4891931
View online: http://dx.doi.org/10.1063/1.4891931
View Table of Contents: http://scitation.aip.org/content/aip/journal/jcp/141/7?ver=pdfcov
Published by the AIP Publishing

Effect of hydrophobic mismatch on domain formation and peptide sorting in the multicomponent lipid bilayers in the presence of immobilized peptides

Qing Liang,[1,2,a)] Qing-Yan Wu,[1] and Zhi-Yong Wang[3]
[1]*Center for Statistical and Theoretical Condensed Matter Physics and Department of Physics, Zhejiang Normal University, Jinhua 321004, People's Republic of China*
[2]*Department of Physics, Ningbo University, Ningbo 315211, People's Republic of China*
[3]*School of Optoelectronic Information, Chongqing University of Technology, Chongqing 400054, People's Republic of China*

(Received 27 January 2014; accepted 15 July 2014; published online 15 August 2014)

In the plasma membranes, many transmembrane (TM) proteins/peptides are anchored to the underlying cytoskeleton and/or the extracellular matrix. The lateral diffusion and the tilt of these proteins/peptides may be greatly restricted by the anchoring. Here, using the coarse-grained molecular dynamics simulation, we investigated the domain formation and peptide sorting in the ternary lipid bilayers in the presence of the immobilized peptide-grid and peptide-cluster. We mainly focused on examining the combining effect of the peptide immobilization and hydrophobic mismatch on the domain formation and peptide sorting in the lipid bilayers. Compared to the lipid bilayers inserted with free TM peptides, our results showed that, because of the tilt restriction imposed on the peptides, the hydrophobic mismatch effect more significantly influences the domain size, the dynamics of domain formation, and the peptide sorting in our systems. Our results provide some theoretical insights into understanding the formation of nanosized lipid rafts, the protein sorting in the lipid rafts and the interaction between the cytoskeleton, the extracellular matrix, and the plasma membranes.
 [http://dx.doi.org/10.1063/1.4891931]

I. INTRODUCTION

The plasma membranes are two-dimensional well-organized bilayers composed of thousands of kinds of lipids and proteins. It is widely accepted that the nanosized and highly dynamic lipid rafts are important structural and functional units in the plasma membranes.[1,2] However, because of the structural complexity and the dynamic property of the plasma membranes, direct observation of the microscopic structure and the components of the lipid rafts *in vivo* is still challenging. Thus, the model membranes, such as the multicomponent supported lipid bilayers,[3–5] the giant unilamellar vesicles (GUV),[6,7] and the isolated plasma membranes,[8–10] are the substitutional systems for the investigation of the microscopic structure and dynamic property of natural plasma membranes. For example, in the ternary model membranes composed of the saturated lipid, the unsaturated lipid, and cholesterol, under certain conditions of temperature and molar ratio of components, it was found two kinds of coexisting liquid domains: the liquid-disordered (ld) domain enriched in the unsaturated lipid and the liquid-ordered (lo) domain enriched in the saturated lipid and cholesterol. In particular, the lo domain is believed to be similar in components to the lipid rafts in the natural plasma membranes.[11] In most of the model membranes, the lipid domains are sub-micrometer to micrometer in size so that they can be conveniently observed with the conventional microscopies such as the confocal microscopy.[12] However, the size of the lipid rafts in the natural plasma membranes is usually 10–200 nm,[13,14] which is much smaller than the size of the lipid domains in the model membranes. This difference implies that the mechanism of the domain formation in the natural plasma membranes and in the model membranes may be different. The microscopic mechanism of the formation of the nanosized lipid rafts in the natural plasma membranes is still a big challenge.[14]

Additionally, there are also some differences between the protein/peptide sorting in the model and natural plasma membranes. In the natural plasma membranes, many transmembrane (TM) proteins are localized in the ordered lipid rafts to realize their signaling and trafficking functions.[2,15,16] However, in the model membranes, both theoretical and experimental studies showed that some TM proteins/peptides prefer to reside in the ld domains even though there is a great mismatch between the hydrophobic thickness of the ld domains and the hydrophobic length of the peptides.[17–21] The hydrophobic mismatch effect,[22–28] which is widely believed to be a crucial factor for the protein/peptide sorting in the plasma membranes, does not seem to have influence on the peptide sorting in the model membranes. The reason for the differences of the protein/peptide sorting in the model and natural plasma membranes, especially the actual effect of the hydrophobic mismatch on the protein sorting, should be further explored.

Recently, the development of the super-resolution microscopy provides the possibility for the observation of the microscopic structure and dynamics in the natural plasma

a)Electronic mail: qliang@zjnu.edu.cn

membranes *in vivo*.[29–39] With the application of the super-resolution microscopy in the microscopic structure of the plasma membranes, it is increasingly realized that the plasma membranes are not isolated lipid bilayers but integrated with the underlying cytoskeleton and the extracellular matrix which is a complex network of polysaccharides and proteins.[38–44] Some TM proteins/peptides and lipids are anchored to the cytoskeleton and/or the extracellular matrix. This anchoring remarkably restricts the lateral movement and tilt of the TM proteins, and may further influence the peptide/protein sorting and the domain formation in the plasma membranes.[5,41–47] However, in previous work, most of the model membranes are isolated membranes where both the lipids and TM proteins/peptides can freely diffuse in the lateral plane and tilt in the normal direction of the membrane. Therefore, it is reasonable to attribute one of the reasons for the structural and dynamical differences between the model membranes and the natural plasma membranes to the cytoskeleton and/or the extracellular matrix anchoring to the TM proteins. Motivated by these experimental findings, some theoretical efforts have been devoted to revealing the effect of disordered pinnings (immobilized lipids or peptides) on the domain formation in the lipid bilayers.[48–52] It was found that the introduction of the pinnings can dramatically influence the diffusion behaviour of the lipids and slow down the coarsening process of the small lipid domains into the micrometer-sized domains. This result is consistent with the theoretical studies of the phase separation of the ordinary binary fluid with quenched disorder.[53–55]

In this paper, to reveal the combining effect of the cytoskeleton and the extracellular matrix anchoring to the TM proteins/peptides and the hydrophobic mismatch between TM proteins/peptides and lipids on the domain formation and peptide sorting in the plasma membranes, we examined the microscopic structures of the lipid bilayers in the presence of the immobilized peptide-grid and peptide-cluster using the coarse-grained molecular dynamics (MD) simulation.[56–60] In the lipid bilayer inserted with the peptide-grid, we focused on examining the combining effect of TM protein immobilization and hydrophobic mismatch on the domain formation in the membrane. We found that, when the hydrophobic length of the peptides is much smaller than the hydrophobic thickness of the lipid bilayer, each peptide is surrounded by a small ld domain and no large ld domain is formed; whereas, when the hydrophobic length of the peptides is comparable to or larger than the hydrophobic thickness of the lipid bilayer, the lipid bilayer is macroscopically separated into two large lo and ld domains and no small lipid domains are formed. In the lipid bilayer in the presence of the immobilized peptide-cluster, we concentrated on revealing the hydrophobic mismatch effect on the sorting of the immobilized peptide-clusters in the membranes. We found that, with the increase in the peptide length, the peptide-cluster tends to transfer from the ld domain into the lo domain. These results showed that, because of the restriction of the lateral diffusion and tilt imposed on the peptides, the hydrophobic mismatch effect plays a more important role in the domain formation and the peptide sorting in the lipid bilayers in the presence of the immobilized peptides.

II. MODEL AND METHODS

A. System setup

Based on the method proposed in Ref. 61, we first built up a ternary lipid bilayer consisting of 828 saturated dipalmitoylphosphatidylcholine (DPPC), 540 unsaturated dilinoleyl-PC (DLiPC), and 576 cholesterol molecules. Thus, the molar ratio of DPPC:DLiPC:cholesterol is about 0.42:0.28:0.30. The lipid bilayer was solvated by 12 600 coarse-grained water beads. The size of the simulation box was about 22.2 nm in x, y directions (bilayer plane) and 7.2 nm in z (bilayer normal) direction. The periodic boundary conditions were used in all three directions. To obtain a disordered lipid bilayer as the initial state for the following simulations, we simulated the ternary lipid bilayer at a high temperature of 350 K for 800 ns after the procedures of energy minimization and equilibration.

When the disordered ternary lipid bilayer was formed, 16 WALP peptides were inserted into the lipid bilayer. The reason for the choice of WALP peptide is that the hydrophobic length of WALP can be continuously changed to systematically explore the hydrophobic mismatch effect on the domain formation and peptide sorting in the lipid bilayer. We considered two different peptide distributing states. In the first state, the peptides were regularly arranged as a 4×4 grid with the grid-spacing $\sim$5.5 nm. In the second state, the peptides were compactly aggregated as a peptide-cluster. In both of these two distributing states, the position of each peptide was fixed by imposing a strong harmonic position restraint with the force constant 1000 kJ mol^{-1} nm^{-2} on the coarse-grained beads along the peptide backbone throughout the whole simulation. Additionally, this restraint also prevented the tilt of the peptides and kept the peptides always normal to the bilayer plane throughout the simulations. Because the radius of the model peptide WALP is small, when the peptides were distributed as a regular grid, after the energy minimization and equilibration, neither the lipid (DPPC and DLiPC) nor cholesterol molecules were overlapped by the peptides. However, when the peptides were aggregated as a cluster, a number of the lipid and cholesterol molecules would be overlapped by the cluster during the peptide insertion. These overlapped molecules should be removed before the simulation and the final numbers of DPPC, DLiPC, and cholesterol molecules were reduced to 779, 507, 546, respectively. To examine the hydrophobic mismatch effect, the WALP length was changed by changing the amino acid number of the hydrophobic part of the peptide. We used four kinds of WALPs: WALP16 (GWW(LA)$_5$WWA), WALP23 (GWW(LA)$_8$LWWA), WALP27 (GWW(LA)$_{10}$LWWA), and WALP31 (GWW(LA)$_{12}$LWWA). The hydrophobic lengths of these four kinds of peptides are $\sim$1.50 nm, 2.55 nm, 3.15 nm, and 3.75 nm, respectively.[26]

Additionally, to estimate the finite size effect on the domain formation in the membrane, we also examined the domain formation in larger membranes in the presence of WALP16-grid and WALP27-grid, respectively. The larger membranes were constructed by copying the corresponding above-constructed membranes two times in both the lateral x and y directions (i.e., the area of the new membrane is

four times larger than the area of the corresponding above-constructed membrane.).

B. Molecular simulation with the MARTINI force field

We used the Gromacs package (version 4.6)[62–64] to perform the MD simulations in this work. The MARTINI force field was used to coarse grain the lipid, cholesterol, water, and WALP molecules. In the MARTINI force field, 3–4 non-hydrogen atoms are mapped into one interaction bead and four water molecules are represented by a coarse-grained water bead.[56–59] In addition, it was found that the molecules diffuse about four times faster in the MARTINI model than in the real system. Therefore, to compare with the experimental results, the simulation time should be multiplied by a time scaling factor of 4.[21,56,61] In this work, however, all of the times mentioned are the simulation times except for being pointed out explicitly.

In the coarse-grained MD simulations, the integration time step of the simulations was set to 20 fs. For the non-bonded interactions, we used the standard parameter scheme of the MARTINI model: the Coulomb interaction was shifted to zero between 0 and 1.2 nm, the Lennard-Jones interaction was shifted to zero between 0.9 and 1.2 nm, and the relative dielectric constant is 15. The constant particle number, pressure, and temperature (NpT) ensemble was used in the simulations. The lipid, cholesterol, peptide, and water molecules were separately coupled to a heat bath with a relaxation time $\tau_T = 1.5$ ps to maintain the system temperature at 310 K. The bilayer (xy) plane and the normal (z) direction were separately coupled to a pressure bath of 1 bar with a relaxation time $\tau_p = 3.0$ ps. The compressibility was set as 3×10^{-5} bar^{-1} in both lateral and normal directions to ensure that the lipid bilayer is tensionless.[65] All the systems simulated in this work and the corresponding simulation and effective times are summarized in Table I.

C. Data analysis

The simulation snapshots in this work were produced by the visualization software VMD.[66] Because the thicknesses of the lo and ld domains are different, we analyzed the two-dimensional thickness profile of the lipid bilayer to assistantly demonstrate the property of the lo and ld domains using a grid-based membrane analysis tool GridMAT-MD.[67] To reveal the effect of the immobilized peptides on the lateral diffusion of the lipids and the dynamics of the domain formation, we calculated the mean square displacement (MSD) of the lipids in the bilayer plane with the analysis tool g_msd in Gromacs. To examine the demixing process of the domain formation, we calculated the number of DPPC–DLiPC contacts (n_{pl}) and the number of DLiPC–DLiPC contacts (n_{ll}) with g_mindist in Gromacs. The fraction of the contacts of DPPC–DLiPC, $f_{pl} = n_{pl}/(n_{pl} + n_{ll})$, was used to characterize the degree of the separation between DPPC and DLiPC during the simulations.[65] The smaller the fraction of DPPC–DLiPC contacts (f_{pl}) is, the more strongly the two kinds of lipids are separated. To examine the peptide sorting in the lipid domains, we also calculated the number of contacts between WALPs and DPPCs (n_{wp}) and the number of contacts between WALPs and DLiPCs (n_{wl}). The fraction of the WALP–DPPC contacts, $f_{wp} = n_{wp}/(n_{wp} + n_{wl})$, described the sorting of WALPs in the lipid domains. The larger the fraction of the WALP–DPPC contacts (f_{wp}) is, the more preferentially the peptides are distributed in the DPPC-enriched lo domain. Here, we supposed that two lipids or a lipid and a peptide contacted with each other if the distance between the lipid headgroups or the distance between the lipid headgroups and the peptides was less than 1.0 nm.[65] To examine the structure of the lipid domains, we calculated the two dimensional (2D) radial distribution functions (RDFs) between the phosphate headgroup beads of the lipids with g_rdf in Gromacs.

Additionally, using the Bennett Acceptance Ratio (BAR) method,[68] we calculated the free energy (ΔG_{lo}) of extracting a peptide from a lo lipid bilayer patch containing 368 DPPC, 224 cholesterol, and 4736 water molecules and the free energy (ΔG_{ld}) of extracting a peptide from a ld lipid bilayer patch containing 336 DLiPC, 32 DPPC, 80 cholesterol, and 4800 water molecules, respectively. Here, the peptide is also immobilized and forbidden to tilt. If $\Delta G_{lo} > \Delta G_{ld}$, the peptide prefers to reside in the lo domain; otherwise, the peptide prefers to reside in the ld domain. The difference of these two free energies, $\Delta G_{lo/ld} = \Delta G_{lo} - \Delta G_{ld}$, is the free energy of transferring a peptide from the lo domain to the ld domain.[21] For the details of the free energy calculation, we refer the readers to Ref. 21.

TABLE I. Overview of the simulation systems and the corresponding simulation/effective times.

No.	System	Simulation time/effective time (μs)
I	Lipid bilayer without WALP	20/80
II	I + WALP16-grid	25/100
III	I + WALP23-grid	25/100
IV	I + WALP27-grid	25/100
V	I + WALP31-grid	25/100
VI	I + WALP16-cluster	20/80
VII	I + WALP23-cluster	20/80
VIII	I + WALP27-cluster	20/80
IX	I + WALP31-cluster	20/80
X	4× II	12/48
XI	4× IV	12/48

III. RESULTS AND DISCUSSION

A. Phase separation of the ternary DPPC/DLiPC/cholesterol lipid bilayer without peptide

The previous work showed that the lipid bilayer composed of DPPC, DLiPC, and cholesterol with the molar ratio of 0.42:0.28:0.30 can be spontaneously separated into the lo and ld domains at 295 K.[61] In this paper, to simulate the domain formation in plasma membrane *in vivo* more realistically, we set the system temperature at the physiological temperature 37°C(310 K). Recently, Janosi *et al.* found that a similar lipid bilayer composed of DPPC, DLiPC, and cholesterol with the molar ratio 5:3:2 can be also separated into the lo and ld domains at a high temperature of 311 K (38°C).[69] Here, to offer a reference for the following simulations, we simulated

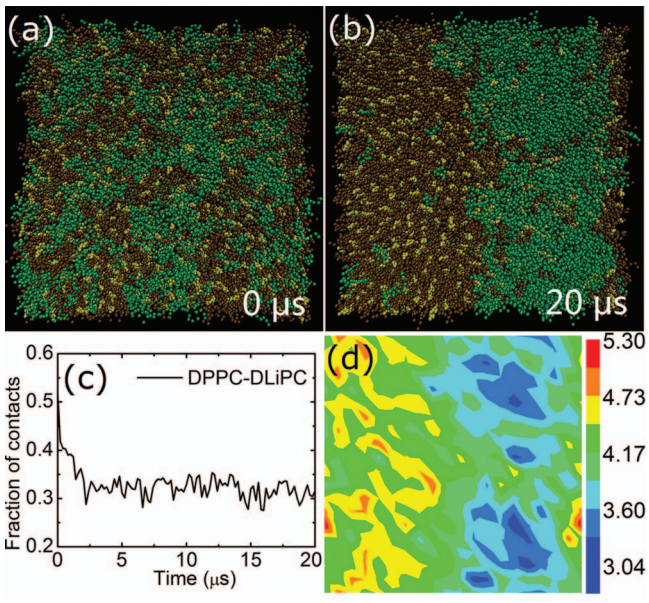

FIG. 1. (a) Top view of the initial disordered structure of a ternary lipid bilayer composed of DPPC (ochre), DLiPC (turquoise), and cholesterol (yellow). Note that this color scheme is used throughout the paper. (b) Top view of the final snapshot of the 20 μs simulation of the ternary lipid bilayer. (c) Time evolution of the fraction of contacts between DPPC and DLiPC. (d) Two-dimensional profile of the bilayer thickness of the snapshot shown in (b).

the phase separation of the DPPC/DLiPC/cholesterol (the molar ratio 0.42:0.28:0.30) lipid bilayer without peptides at 310 K and the results are shown in Fig. 1. We find that the lipid bilayer considered in this work can be also spontaneously separated into the lo and ld domains at 310 K (Figs. 1(a) and 1(b)). Additionally, from the time evolution of the fraction of the DPPC–DLiPC contacts shown in Fig. 1(c), we find that the phase separation is completed within the initial 2 μs of the simulation and the two lipid domains stably exist during the subsequent simulation time. From Fig. 1(d), we can find that the lo domain thickness which is measured by the headgroup-headgroup distance of DPPCs is ~4.4 nm, whereas the ld domain thickness is ~3.7 nm. It is notable that the hydrophobic thicknesses of the lo and ld domains are about 1 nm smaller than the thicknesses of the lo and ld domains, respectively,[65] i.e., they are ~3.4 nm and 2.7 nm, respectively.

B. Domain formation in the lipid bilayers in the presence of the immobilized peptide-grids

We first explored the effect of hydrophobic mismatch between the lipid domains and the single peptide on the domain formation in the lipid bilayer. In the relevant previous studies,[48–51] it was found that, if the immobilized proteins were randomly distributed in the lipid bilayer and showed affinity with one kind of the lipids, the final shape and the size of the lipid domains were greatly determined by the distribution of the proteins. Here, to avoid the influence from the peptide distribution on the domain size, distribution, and shape, the positions of the peptides were fixed as a regular grid to mimic the anchoring of a fictitious regular cytoskeleton network.[52,70] Additionally, the tilt of the peptide was strictly forbidden to mimic the combining restricting effect of the

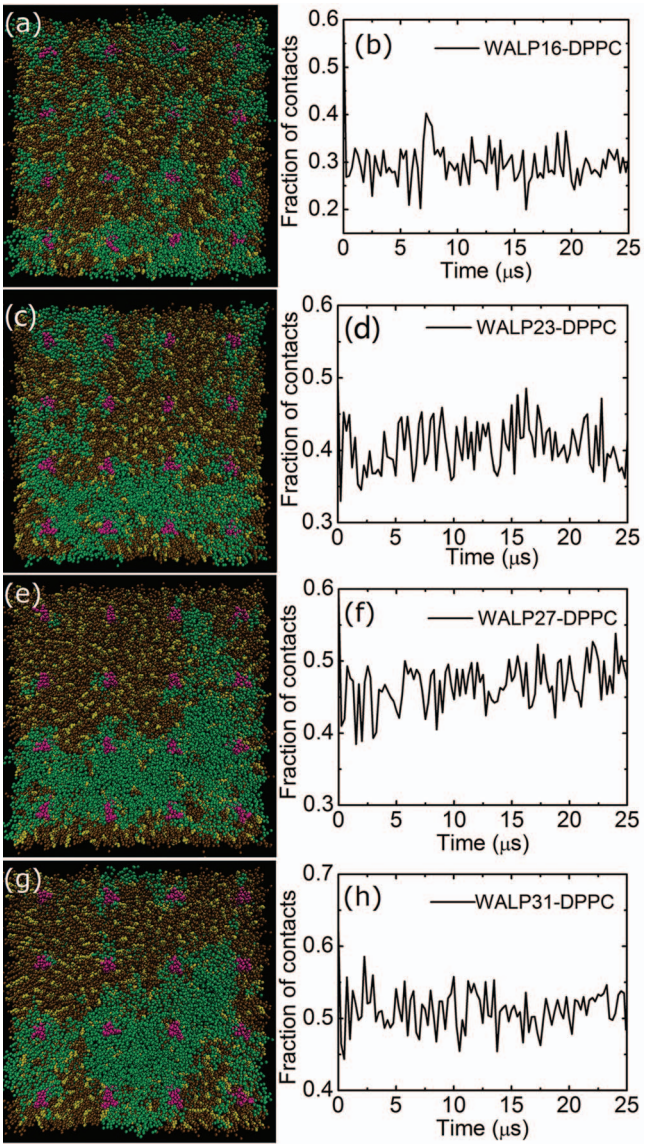

FIG. 2. The final snapshots of the 25 μs simulations of the ternary lipid bilayers in the presence of the immobilized grids of (a) WALP16, (c) WALP23, (e) WALP27, and (g) WALP31 and the corresponding time evolution of the fraction of contacts between WALPs and DPPCs. The WALP peptides are shown in magenta.

cytoskeleton and the extracellular matrix anchoring on the peptide tilt in the natural plasma membranes. The final snapshots of the simulations and the time evolution of the fractions of WALP–DPPC contacts of the lipid bilayers in the presence of immobilized peptide-grids are shown in Fig. 2 with the variation of the peptide length.

From Fig. 2(a), we find that each immobilized WALP16 is surrounded by a small ld domain with the domain radius of ~3–5 nm and no large ld domain is formed within the whole simulation time (25 μs). The WALP16–DPPC contact fraction (Fig. 2(b)) also shows that the small ld domains are relatively stable during the whole simulation. In the membrane inserted with the immobilized WALP23-grid (Fig. 2(c)), although some WALP23s are surrounded by small ld domains, the majority of DLiPCs tend to be coalesced into a larger ld domain. However, DLiPCs are packed loosely in the ld domain throughout the 25 μs simulation. From

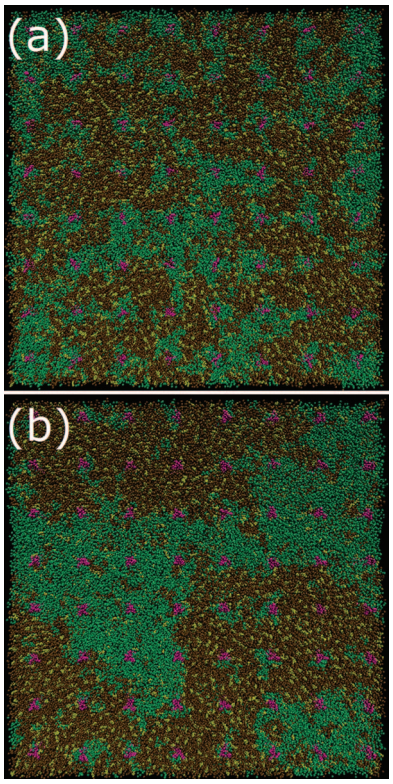

FIG. 3. The final snapshots of the 12 μs simulations of the membranes whose areas are 4 times larger than the areas of the membranes in Fig. 2 in the presence of the immobilized grids of (a) WALP16 and (b) WALP27.

Fig. 2(d), we find that more DPPCs are in contact with the immobilized WALP23s compared to the membrane inserted with WALP16-grid.

When the hydrophobic length of the peptide is further increased (the cases of the WALP27-grid and the WALP31-grid shown in Figs. 2(e)–2(h)), the lipids are separated from each other and large lo and ld domains are formed. From the curves of the fraction of the WALP–DPPC contacts (Figs. 2(f) and 2(h)), we can find that the contacts between WALPs and DPPCs increase with the increase of the length of WALP. WALP31s more preferentially reside in the lo domain than WALP27s. Additionally, due to the pinning of the immobilized peptides, the shape of the lipid domains is not a circle or a stripe but irregular.

In order to examine whether the box size of the system in Fig. 2 is large enough and has no influence on the domain formation, we also simulated larger membranes inserted with the immobilized grids of 64 WALP16s and WALP27s, respectively. The final structures of the larger membranes are shown in Fig. 3. We find that, for both the larger membranes inserted with WALP16-grid and WALP27-grid, the structures of the larger membranes do not show obvious difference to the structures of the corresponding smaller membranes in Fig. 2. Furthermore, the RDFs in Fig. 4 also indicate that, the average radius of the ld domains is about 3.5 nm in both the smaller and the larger membranes inserted with shorter WALP16-grid and the average radius of the macroscopically separated ld domains in the membranes inserted with longer WALP27-grid increases with the increase of the system size. This result is consistent with the finite size effect analysis of a similar system in Ref. 65 and implies that the size of the systems shown in Fig. 2 is large enough and the results are reliable.

It is notable that the domain formation in the lipid bilayers in the presence of immobilized peptide-grids may also be influenced by the peptide density (or the spacing between

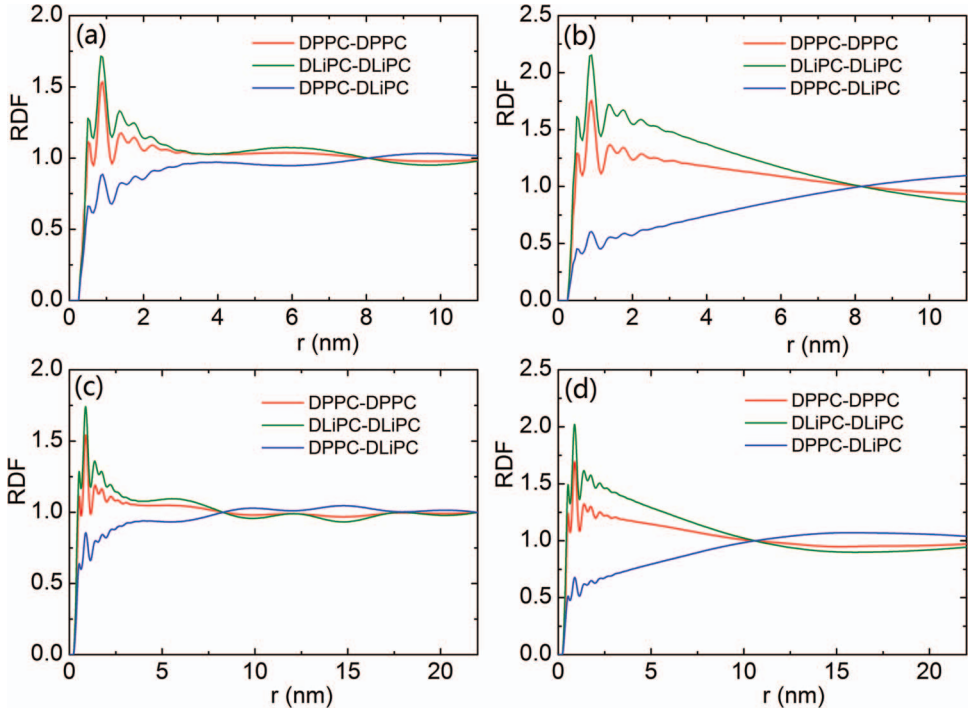

FIG. 4. The two-dimensional radial distribution functions (RDFs) of the lipids in the smaller membranes inserted with immobilized grids consisted of (a) 16 WALP16s and (b) 16 WALP27s and in the larger membranes inserted with immobilized grids consisted of (c) 64 WALP16s and (d) 64 WALP27s. The RDFs were calculated by averaging over the last 1 μs of the simulations, the bin-width is 0.05 nm, and two bilayer leaflets were analyzed separately.

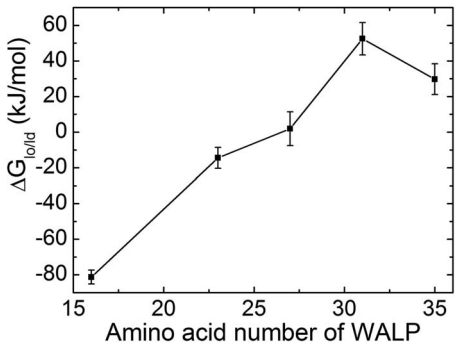

FIG. 5. The free energy of transferring a WALP peptide from a lo lipid bilayer patch to a ld lipid bilayer patch ($\Delta G_{lo/ld}$) with the variation of the amino acid number of WALP.

peptides),[52] temperature, etc. For the membrane inserted with WALP16-grid, a larger peptide spacing may restrain the coalescing of the small ld domains; whereas, for the membrane inserted with longer WALP27-grid or WALP31-grid, the microscopic phase separation is expected to take place and small lipid domains may be formed if the temperature is risen. However, this is beyond the concern of the present study and possibly considered in the future work.

To deeply understand the microscopic mechanism of the influence of the immobilized WALP-grids on the domain formation in the lipid bilayer, the free energy of transferring an immobilized peptide from a lo lipid bilayer patch to a ld lipid bilayer patch ($\Delta G_{lo/ld}$) was calculated and shown in Fig. 5 with the variation of the length (the amino acid number) of the peptide. We find that the transfer free energy of WALP16 from the lo domain to the ld domain is very small (-81.27 ± 3.89 kJ mol^{-1}), which indicates that WALP16 prefers to reside in the ld domain. Because the lipids in the ld domains are packed loosely and disorderedly, the preference of the residence of WALP16 in the ld domain is partially attributed to the enthalpic affinity between the peptides and the ld domains.[21] Additionally, because the hydrophobic length of WALP16 (1.50 nm) matches the hydrophobic thickness of the ld domains (2.7 nm) better than that of the lo domains (3.4 nm), the hydrophobic mismatch effect also plays an important role in the distribution of WALP16 in the ld domains. Undoubtedly, the scattered distribution of the ld domains as shown in Fig. 2(a) will increase the interface and the interfacial energy between the lo and ld domains. However, the increase of the interfacial energy can be completely counteracted by the decrease of the free energy because of the distribution of WALP16 peptides in the ld domains.

With the increase of the hydrophobic length of the peptide, we find that the transfer free energy increases and approaches zero as the amino acid number of the peptide is increased to 27. Thus, in the membranes inserted with immobilized WALP23-grid and the WALP27-grid, if the ld domains are still distributed as shown in Fig. 2(a), although the free energy would either be decreased (the case of the WALP23-grid) or maintain unchanged (the case of the WALP27-grid), the increase of the interfacial energy cannot be completely counteracted by the decrease of the free energy. Therefore, the two kinds of lipids tend to be separated into two large lo and ld domains to reduce the interfacial energy. However, because of the increase in the transfer free energy, the lipids are separated more strongly in the membrane inserted with the WALP27-grid than in the membrane inserted with the WALP23-grid.

As the amino acid number of the peptide is increased to 31, the free energy of transferring a WALP31 from the lo domain to the ld domain becomes a positive value (52.48 ± 9.09 kJ mol^{-1}). This implies that, because the hydrophobic length of WALP31 (3.75 nm) matches the hydrophobic thickness of lo domain much better than that of ld domain, WALP31 prefers to reside in the lo domain due to the hydrophobic mismatch effect. However, if all WALP31s are surrounded by small lo domains, although the transfer free energy is relatively large, the increase of the interfacial energy will exceed the reduction of the free energy. Consequently, the lipids are also separated into two large domains to reduce the interfacial energy in the case of the WALP31-grid.

We further calculated the transfer free energy of WALP35 from the lo domain to the ld domain. Because the hydrophobic length of WALP35 (4.35 nm) is much larger than the hydrophobic thicknesses of both the ld and lo domains, the hydrophobic mismatch effect will become weaker compared to the case of WALP31. Therefore, the transfer free energy of WALP35 is smaller than that of WALP31 as shown in Fig. 5. This reduction of the transfer free energy further proves that the variation of the transfer free energy shown in Fig. 5 is resulted from the variation of hydrophobic mismatch effect.

From Fig. 5 and the above discussion, we find that the hydrophobic mismatch effect, the enthalpy, and the interfacial energy jointly dominate the domain formation in the lipid bilayers inserted with the immobilized peptide-grids in the present work. The final domain size is determined by the competition of these effects. Additionally, the hydrophobic mismatch effect can also influence the sorting of the immobilized peptides in the lipid domains.

In order to reveal the influence of the immobilized peptide-grid on the diffusion of the lipids, we calculated the MSD of DPPC and DLiPC in the lateral plane of the lipid bilayers inserted with the immobilized peptide-grids and the results are shown in Fig. 6. We find that the lateral diffusion of DPPC is barely affected by the immobilized peptide-grid, whereas DLiPCs feel a relatively larger influence from the immobilized peptide-grid and the diffusion of DLiPC is slowed down by a factor of $\sim$2 in the long-time limit. We can also observe this effect by examining the time of the domain formation in the lipid bilayers. For example, in the lipid bilayer inserted with the immobilized WALP31-grid, the time of the formation of the large domains is $\sim 5\ \mu$s, whereas it is $\sim 2\ \mu$s in the ternary lipid bilayer without peptides. This observation agrees well with the results of previous relevant studies.[48–55] Additionally, the influence of the hydrophobic mismatch effect (or the peptide length) on the lateral diffusion of lipids is negligible.

C. Sorting of the immobilized peptide-cluster in the lipid bilayers

In the natural plasma membrane, larger TM proteins are more ubiquitous than the single peptide. To explore the

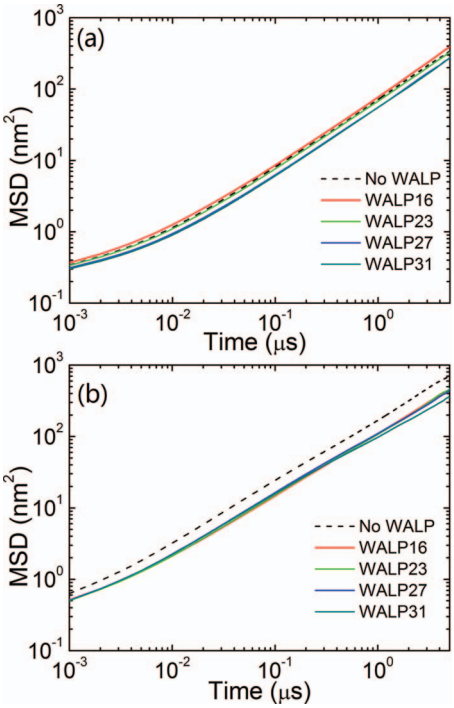

FIG. 6. The mean square displacements (MSD) of (a) DPPC and (b) DLiPC in the lateral plane of the lipid bilayers inserted with the immobilized WALP-grids in comparison with the MSD of DPPC and DLiPC in the lipid bilayers without peptides. The last 5 μs of the simulations is analyzed.

sorting of large proteins in the plasma membrane, we aggregated the 16 peptides into an immobilized cluster to mimic the real proteins in plasma membranes. The advantage of the model peptide-cluster over the real proteins is that the hydrophobic length of the peptide-cluster can be conveniently changed to explore the hydrophobic mismatch effect on the protein sorting in the membrane.

Fig. 7 shows the final snapshots of the 20 μs simulations and the time evolution of the WALP–DPPC contact fractions of the lipid bilayers inserted with the immobilized peptide-cluster with the variation of the peptide length. We find that the lipid bilayers are always separated into large lo and ld domains regardless of the hydrophobic length of the peptide. However, the sorting of the peptide-cluster is significantly affected by the effect of hydrophobic mismatch between the peptides and the lipid domains. In the membranes inserted with the WALP16-cluster and the WALP23-cluster, the hydrophobic length of the peptide-clusters is short. Therefore, both the WALP16-cluster and the WALP23-cluster stably reside in the thinner ld domains due to the effects of the strong hydrophobic mismatch and enthalpy (Figs. 7(a)–7(d)).

In the membrane inserted with the immobilized WALP27-cluster, the peptide-cluster resides on the boundary of the lo and ld domains in the later period of the simulation (Fig. 7(e)). However, from Fig. 7(f), we find that the fraction of contacts between WALP27 and DPPC is very small (0.1–0.3) in the earlier stage of the simulation, which indicates that the WALP27-cluster is surrounded by the ld domain in most of the earlier simulation time. This can be understood as follows: on the one hand, because WALP27s prefer to distribute in the ld domains due to the effect of enthalpy, the

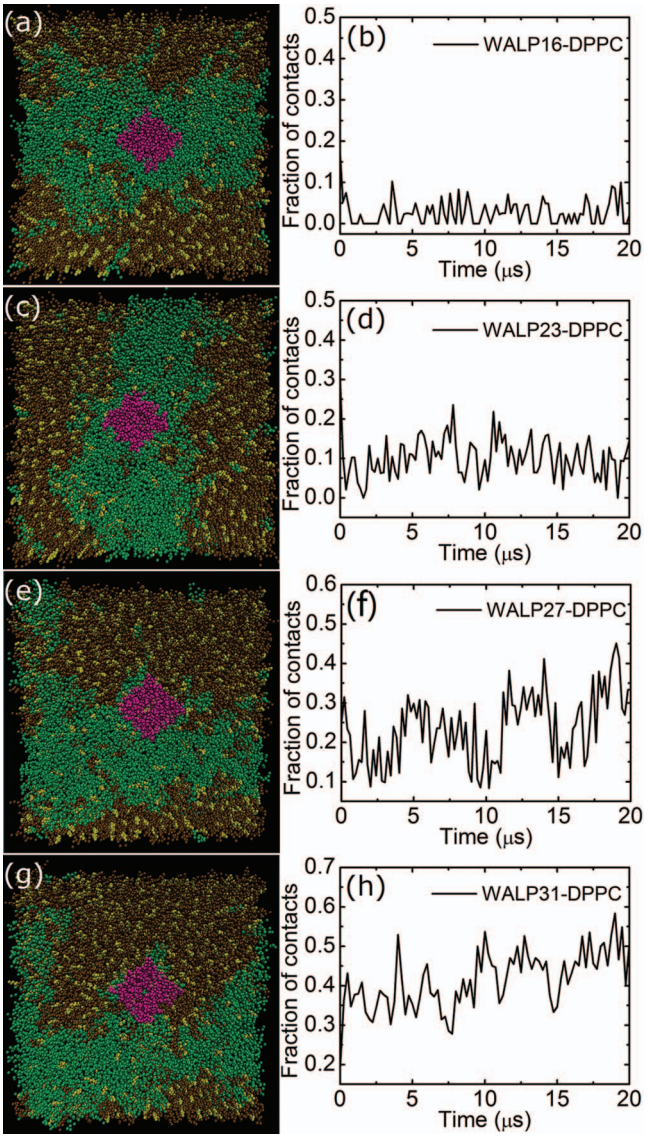

FIG. 7. The final snapshots of 20 μs simulations of the ternary lipid bilayers in the presence of the immobilized clusters of (a) WALP16, (c) WALP23, (e) WALP27, and (g) WALP31 and the corresponding time evolution of the fraction of the contacts between WALPs and DPPCs.

peptide-cluster provides a core for the growth of the ld domain and DLiPCs aggregate around the peptide-cluster in the earlier stage of simulation; on the other hand, the hydrophobic length of WALP27 (3.15 nm) does not well match the hydrophobic thickness of either the ld or the lo domains and the peptides are forbidden to tilt, thus, the shape and the location of the lipid domains are continuously modulated and the WALP27-cluster finally resides on the boundary of the lo and ld domains.

In the membrane inserted with the immobilized WALP31 -cluster, the peptide-cluster also resides near the boundary of the lo and ld domains in the later period of the simulation but tends to distribute in the lo domains (Fig. 7(g)). Additionally, Fig. 7(h) shows that the contacts between WALP31 and DPPC obviously increase during the whole simulation compared to the case of the WALP27-cluster and even exceeds 0.5 at some time (e.g., 4 μs, 17.5 μs, and 19 μs) of the simulation. This means that the WALP31-cluster is much more preferentially

distributed in the lo domains than the shorter WALP-clusters. However, because the free energy of transferring a WALP31 from the lo domain to the ld domain is not large enough, the WALP31-cluster is not able to stably reside in the lo domain but resides near the boundary of the lo and ld domains in most of the simulation time.

Here, the distribution of the peptide-clusters is greatly different to the distribution of the TM proteins in the lipid rafts in the natural plasma membranes. This difference implies that, in the natural plasma membranes, besides the hydrophobic mismatch effect, some other factors (e.g., temperature, electrostatic interaction, etc.) are also very crucial to drive the TM proteins or peptides to reside in the ordered lipid rafts. The microscopic mechanism of the residence of TM proteins in the lipid rafts in the plasma membranes needs more efforts in the future work.

Nevertheless, from Fig. 7, we can find that the hydrophobic mismatch effect obviously influences the distribution of the immobilized peptide-clusters. In most of the previous studies on the interactions between the lipid bilayer and the TM peptides/proteins, the peptides or proteins are mobilizable and can be freely tilted in the normal direction of the bilayer. This means that, when the length of the hydrophobic part of a peptide/protein does not match the hydrophobic thickness of the lipid domain, the peptide/protein can be tilted to (partially) counteract the hydrophobic mismatch effect. This may explain why the hydrophobic mismatch effect is not so important in the sorting of peptides in the membranes inserted with free peptides/proteins[21] as in the lipid bilayer inserted with the immobilized peptides. Obviously, the later system is more realistic in description of the combining restriction of the cytoskeleton and the extracellular matrix anchoring to the lateral diffusion and tilt of the TM proteins in the natural plasma membrane.

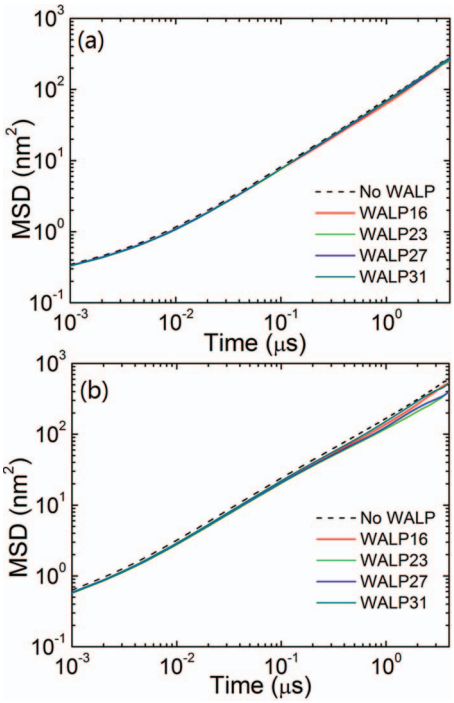

FIG. 8. The mean square displacements (MSD) of (a) DPPC and (b) DLiPC in the lipid bilayers inserted with the immobilized WALP-clusters in comparison with the MSD of DPPC and DLiPC in the lipid bilayers without peptides. The last 4 μs of the simulations is analyzed.

Finally, we calculated the MSD of DPPC and DLiPC in the lateral plane of the lipid bilayers in the presence of the immobilized peptide-cluster (Fig. 8). Different to the cases of the immobilized peptide-grids, both the lateral diffusions of DPPC and DLiPC are not obviously influenced by the immobilized WALP-clusters, and the time for the formation of the large lipid domains ($\sim$2 μs) is close to the time of the domain formation in the ternary lipid bilayer without peptides. Therefore, we can conclude that the scattered distribution of the immobilized peptides has a more significant influence on the lateral diffusion of the lipids and the dynamics of domain formation than the compact distribution.

IV. CONCLUSION

In this work, we mainly examined the effect of hydrophobic mismatch on the domain formation and peptide sorting in the ternary lipid bilayers in the presence of the immobilized peptide-grid and peptide-cluster using the coarse-grained MD simulation. We found that, different to the membranes inserted with the free peptides, the hydrophobic mismatch effect greatly influences the domain formation and peptide sorting in the present system due to the restriction of tilt imposed on the peptides. In addition, the roles of enthalpy and interfacial energy are also not negligible for the domain formation of the lipid bilayer.

In the lipid bilayers in the presence of the regular immobilized peptide-grids, the domain formation is determined by the competition between hydrophobic mismatch effect, enthalpy, and the interfacial energy. In the membrane inserted with shorter immobilized WALP16-grid, the strong hydrophobic mismatch effect together with the enthalpy wins the interfacial energy, all of WALP16s are surrounded by small ld domains and no large domain is formed. For the case of longer peptide-grid, the hydrophobic mismatch effect is weakened and the interfacial energy plays a dominant role in the domain formation and the lipids are separated into two large lo and ld domains.

In the lipid bilayer inserted with the immobilized peptide-cluster, the shorter WALP16-cluster and WALP23-cluster reside in the ld domains due to the strong hydrophobic mismatch effect and the enthalpic preference of the peptides with the ld domains. The longer WALP27-cluster is distributed in the ld domain during the earlier stage of the simulation but finally resides on the boundary of the lo and ld domains due to the effect of the hydrophobic mismatch between the peptide and either the lo or the ld domains. For the WALP31-cluster, although the enthalpy disfavors the residence of the peptides in the lo domain, the WALP31-cluster still tends to distribute in the lo domain due to the strong hydrophobic mismatch effect. Taken together, the hydrophobic mismatch effect and the enthalpy cooperatively dominate the localization of the peptide in the present system.

Additionally, the different distributing states of the immobilized peptides influence the lateral diffusion of the lipids and the dynamics of the domain formation differently. The

scattered distribution of the immobilized peptides influences the lipid diffusion and the lipid domain formation more significantly.

It should be pointed out that, in the natural plasma membranes, the TM proteins may not be completely immobilized and may be partially tilted and the effect of the hydrophobic mismatch on the domain formation and protein sorting may not be so obvious as in the present system. However, as a model system, this work still provided some theoretical insights into understanding the effect of hydrophobic mismatch between TM proteins/peptides and membranes on the domain formation and protein sorting in the natural plasma membranes where the lateral diffusion and tilt of the TM proteins/peptides are remarkably restricted by the cytoskeleton and/or the extracellular matrix anchoring.

ACKNOWLEDGMENTS

This work was supported by National Natural Science Foundation of China (Grant Nos. 11004173 and 11104364), the Starting Research Fund for Doctors from Zhejiang Normal University, the Open Fund of Zhejiang Key Discipline of Applied Nonlinear Science and Technology (Grant No. xkz11209) from Ningbo University, and the Natural Science Foundation Project of Chongqing (Grant No. cstc2012jjA00019). The computational resources provided by the Department of Computer Science and Technology at Zhejiang Normal University is greatly appreciated.

[1]K. Simons and E. Ikonen, Nature (London) **387**, 569 (1997).
[2]D. Lingwood and K. Simons, Science **327**, 46 (2010).
[3]E. Sackmann, Science **271**, 43 (1996).
[4]M. Tanaka and E. Sackmann, Nature (London) **437**, 656 (2005).
[5]F. Roder, O. Birkholz, O. Beutel, D. Paterok, and J. Piehler, J. Am. Chem. Soc. **135**, 1189 (2013).
[6]C. Dietrich, L. Bagatolli, Z. Volovyk, N. Thompson, M. Levi, K. Jacobson, and E. Gratton, Biophys. J. **80**, 1417 (2001).
[7]T. Baumgart, S. T. Hess, and W. W. Webb, Nature (London) **425**, 821 (2003).
[8]T. Baumgart, A. T. Hammond, P. Sengupta, S. T. Hess, D. A. Holowka, B. A. Baird, and W. W. Webb, Proc. Natl. Acad. Sci. U.S.A. **104**, 3165 (2007).
[9]D. Lingwood, J. Ries, P. Schwille, and K. Simons, Proc. Natl. Acad. Sci. U.S.A. **105**, 10005 (2008).
[10]H.-J. Kaiser, D. Lingwood, I. Levental, J. L. Sampaio, L. Kalvodova, L. Rajendran, and K. Simons, Proc. Natl. Acad. Sci. U.S.A. **106**, 16645 (2009).
[11]G. W. Feigenson, Biochim. Biophys. Acta, Biomembr. **1788**, 47 (2009).
[12]E. L. Elson, E. Fried, J. E. Dolbow, and G. M. Genin, Annu. Rev. Biophys. **39**, 207 (2010).
[13]L. J. Pike, J. Lipid Res. **47**, 1597 (2006).
[14]L. J. Pike, J. Lipid Res. **50**, S323 (2009).
[15]P. Sharma, R. Varma, R. Sarasij, Ira, K. Gousset, G. Krishnamoorthy, M. Rao, and S. Mayor, Cell **116**, 577 (2004).
[16]K. G. N. Suzuki, R. S. Kasai, K. M. Hirosawa, Y. L. Nemoto, M. Ishibashi, Y. Miwa, T. K. Fujiwara, and A. Kusumi, Nat. Chem. Biol. **8**, 774 (2012).
[17]M. E. Fastenberg, H. Shogomori, X. Xu, D. A. Brown, and E. London, Biochemistry **42**, 12376 (2003).
[18]K. Bacia, C. G. Schuette, N. Kahya, R. Jahn, and P. Schwille, J. Biol. Chem. **279**, 37951 (2004).
[19]A. T. Hammond, F. A. Heberle, T. Baumgart, D. Holowka, B. Baird, and G. W. Feigenson, Proc. Natl. Acad. Sci. U.S.A. **102**, 6320 (2005).
[20]H. Shogomori, A. T. Hammond, A. G. Ostermeyer-Fay, D. J. Barr, G. W. Feigenson, E. London, and D. A. Brown, J. Biol. Chem. **280**, 18931 (2005).
[21]L. V. Schäfer, D. H. de Jong, A. Holt, A. J. Rzepiela, A. H. de Vries, B. Poolman, J. A. Killian, and S. J. Marrink, Proc. Natl. Acad. Sci. U.S.A. **108**, 1343 (2011).
[22]F. J.-M. de Meyer, M. Venturoli, and B. Smit, Biophys. J. **95**, 1851 (2008).
[23]D. A. Pantano and M. L. Klein, J. Phys. Chem. B **113**, 13715 (2009).
[24]B. West, F. L. Brown, and F. Schmid, Biophys. J. **96**, 101 (2009).
[25]H.-J. Kaiser, A. Orłowski, T. Róg, T. K. M. Nyholm, W. Chai, T. Feizi, D. Lingwood, I. Vattulainen, and K. Simons, Proc. Natl. Acad. Sci. U.S.A. **108**, 16628 (2011).
[26]T. Kim and W. Im, Biophys. J. **99**, 175 (2010).
[27]E. Strandberg, S. Esteban-Martín, A. S. Ulrich, and J. Salgado, Biochim. Biophys. Acta, Biomembr. **1818**, 1242 (2012).
[28]F. A. Heberle, R. S. Petruzielo, J. Pan, P. Drazba, N. Kučerka, R. F. Standaert, G. W. Feigenson, and J. Katsaras, J. Am. Chem. Soc. **135**, 6853 (2013).
[29]E. Betzig, G. H. Patterson, R. Sougrat, O. W. Lindwasser, S. Olenych, J. S. Bonifacino, M. W. Davidson, J. Lippincott-Schwartz, and H. F. Hess, Science **313**, 1642 (2006).
[30]C. Eggeling, C. Ringemann, R. Medda, G. Schwarzmann, K. Sandhoff, S. Polyakova, V. N. Belov, B. Hein, C. von Middendorff, A. Schönle, and S. W. Hell, Nature (London) **457**, 1159 (2009).
[31]K. Simons and M. J. Gerl, Nat. Rev. Mol. Cell Biol. **11**, 688 (2010).
[32]C. Kuo and R. M. Hochstrasser, J. Am. Chem. Soc. **133**, 4664 (2011).
[33]D. M. Owen, D. J. Williamson, A. Magenau, and K. Gaus, Nat. Commun. **3**, 1256 (2012).
[34]A. Toulmay and W. A. Prinz, J. Cell Biol. **202**, 35 (2013).
[35]M. P. Clausen and B. C. Lagerholm, Nano Lett. **13**, 2332 (2013).
[36]E. Klotzsch and G. J. Schütz, Philos. Trans. R. Soc. B **368**, 20120033 (2013).
[37]J. C. Chang and S. J. Rosenthal, ACS Chem. Neurosci. **3**, 737 (2012).
[38]D. M. Owen, A. Magenau, D. Williamson, and K. Gaus, BioEssays **34**, 739 (2012).
[39]J. F. Frisz, K. Lou, H. A. Klitzing, W. P. Hanafin, V. Lizunov, R. L. Wilson, K. J. Carpenter, R. Kim, I. D. Hutcheon, J. Zimmerberg, P. K. Weber, and M. L. Kraft, Proc. Natl. Acad. Sci. U.S.A. **110**, E613 (2013).
[40]P. Lajoie and I. R. Nabi, Int. Rev. Cell Mol. Biol. **282**, 135 (2010).
[41]N. L. Andrews, K. A. Lidke, J. R. Pfeiffer, A. R. Burns, S. Bridget, J. M. Oliver, and D. S. Lidke, Nat. Cell Biol. **10**, 955 (2008).
[42]G. Chichili and W. Rodgers, Cell. Mol. Life Sci. **66**, 2319 (2009).
[43]D. H. de Jong, C. A. Lopez, and S. J. Marrink, Faraday Discuss. **161**, 347 (2013).
[44]B. Alberts, A. Johnson, J. Lewis, M. Raff, K. Roberts, and P. Walter, in *Molecular Biology of the Cell*, 5th ed. (Garland Science, New York, 2007), pp. 629–650.
[45]J. Dinic, P. Ashrafzadeh, and I. Parmryd, Biochim. Biophys. Acta, Biomembr. **1828**, 1102 (2013).
[46]M. V. Gudheti, N. M. Curthoys, T. J. Gould, D. Kim, M. S. Gunewardene, K. A. Gabor, J. A. Gosse, C. H. Kim, J. Zimmerberg, and S. T. Hess, Biophys. J. **104**, 2182 (2013).
[47]F. Heinemann, S. K. Vogel, and P. Schwille, Biophys. J. **104**, 1465 (2013).
[48]T. Witkowski, R. Backofen, and A. Voigt, Phys. Chem. Chem. Phys. **14**, 14509 (2012).
[49]T. Fischer, H. Jelger Risselada, and R. L. C. Vink, Phys. Chem. Chem. Phys. **14**, 14500 (2012).
[50]J. Ehrig, E. P. Petrov, and P. Schwille, Biophys. J. **100**, 80 (2011).
[51]B. B. Machta, S. Papanikolaou, J. P. Sethna, and S. L. Veatch, Biophys. J. **100**, 1668 (2011).
[52]T. Fischer and R. L. C. Vink, J. Chem. Phys. **134**, 055106 (2011).
[53]M. Laradji and G. MacNevin, J. Chem. Phys. **119**, 2275 (2003).
[54]G. S. Grest and D. J. Srolovitz, Phys. Rev. B **32**, 3014 (1985).
[55]M. F. Gyure, S. T. Harrington, R. Strilka, and H. E. Stanley, Phys. Rev. E **52**, 4632 (1995).
[56]S. J. Marrink, H. J. Risselada, S. Yefimov, D. P. Tieleman, and A. H. de Vries, J. Phys. Chem. B **111**, 7812 (2007).
[57]L. Monticelli, S. K. Kandasamy, X. Periole, R. G. Larson, D. P. Tieleman, and S. J. Marrink, J. Chem. Theory Comput. **4**, 819 (2008).
[58]X. Periole, and S.-J. Marrink, in *Biomolecular Simulations*, Methods in Molecular Biology Vol. **924**, edited by L. Monticelli, and E. Salonen (Humana Press, 2013), pp. 533–565.
[59]S. J. Marrink and D. P. Tieleman, Chem. Soc. Rev. **42**, 6801 (2013).
[60]W. D. Bennett and D. P. Tieleman, Biochim. Biophys. Acta, Biomembr. **1828**, 1765 (2013).
[61]H. J. Risselada and S. J. Marrink, Proc. Natl. Acad. Sci. U.S.A. **105**, 17367 (2008).
[62]D. Van Der Spoel, E. Lindahl, B. Hess, G. Groenhof, A. E. Mark, and H. J. C. Berendsen, J. Comput. Chem. **26**, 1701 (2005).
[63]B. Hess, C. Kutzner, D. van der Spoel, and E. Lindahl, J. Chem. Theory Comput. **4**, 435 (2008).

[64]S. Pronk, S. Páll, R. Schulz, P. Larsson, P. Bjelkmar, R. Apostolov, M. R. Shirts, J. C. Smith, P. M. Kasson, D. van der Spoel, B. Hess, and E. Lindahl, Bioinformatics **29**, 845 (2013).
[65]J. Domański, S. J. Marrink, and L. V. Schäfer, Biochim. Biophys. Acta, Biomembr. **1818**, 984 (2012).
[66]W. Humphrey, A. Dalke, and K. Schulten, J. Mol. Graphics **14**, 33 (1996).
[67]W. J. Allen, J. A. Lemkul, and D. R. Bevan, J. Comput. Chem. **30**, 1952 (2009).
[68]C. H. Bennett, J. Comput. Phys. **22**, 245 (1976).
[69]L. Janosi, Z. Li, J. F. Hancock, and A. A. Gorfe, Proc. Natl. Acad. Sci. U.S.A. **109**, 8097 (2012).
[70]M. J. Saxton, Biophys. J. **55**, 21 (1989).